

This article may be downloaded for personal use only. Any other use requires prior permission of the author and AIP Publishing.

The following article appeared in *American Journal of Physics* 81, 104 (2013); and may be found at <https://doi.org/10.1119/1.4765628>

Wave transmission through periodic, quasiperiodic, and random one-dimensional finite lattices

Braulio Gutiérrez-Medina^{a)}

División de Materiales Avanzados, Instituto Potosino de Investigación Científica y Tecnológica, San Luis Potosí, SLP, 78216, Mexico

(Received 26 April 2012; accepted 19 October 2012)

The quantum mechanical transmission probability is calculated for one-dimensional finite lattices with three types of potentials: periodic, quasiperiodic, and random. When the number of lattice sites included in the computation is systematically increased, distinct features in the transmission probability vs. energy diagrams are observed for each case. The periodic lattice gives rise to allowed and forbidden transmission regions that correspond to the energy band structure of the infinitely periodic potential. In contrast, the transmission probability diagrams for both quasiperiodic and random lattices show the absence of well-defined band structures and the appearance of wave localization effects. Using the average transmissivity concept, we show the emergence of exponential (Anderson) and power-law bounded localization for the random and quasiperiodic lattices, respectively. © 2013 American Association of Physics Teachers. [<http://dx.doi.org/10.1119/1.4765628>]

I. INTRODUCTION

The quantum mechanical problem of a moving particle in the presence of a periodic potential (composed of a succession of identical potential barriers) is at the basis of solid state physics—a field where “quantum mechanics has scored some of its greatest triumphs.¹” In the classroom, using this problem as a model for the electron in a crystal lattice helps students appreciate how the wave nature of matter directly leads to the existence of an energy band structure, a concept that in turn explains the distinction between conductors and insulators.

In the past few decades, there has been a continuing interest in the study of wave propagation in non-periodic structures. This area of research was sparked in 1958 with the finding by P. W. Anderson that quantum transport can be arrested by the presence of a random potential,² an effect that has been referred to as “Anderson localization.” Anderson localization depends on dimension. In one and two dimensions, an arbitrarily small degree of disorder leads to localization of all quantum states, provided that the system is sufficiently large. In three dimensions, however, the localized states occur only for energies below a critical value that depends on the disorder strength.³

An unexpected turn in the field of transport in non-periodic lattices came with the 1982 discovery by D. Shechtman of quasicrystals—structures that possess long-range order but do not have the translational symmetry of crystals.⁴ The diffraction patterns of these materials display sharp peaks (reflecting long-range order) but are fivefold symmetric, which is inconsistent with a periodic lattice.^{5,6} Analysis of the electronic states in 1D-quasiperiodic model systems showed that the wavefunctions are quasi-localized or weakly localized, meaning that the decay at long distances is bounded by a power law rather than an exponential.^{7,8}

Although originally developed within the context of quantum transport in solid-state materials, wave localization studies soon extended to include localization of classical waves. This approach has made it easier to compare experiments and theoretical models on localization, because the often obscuring effects of electron interactions are absent. Using classical waves, it is possible to measure localization in a

material by determining how the transmission coefficient scales with sample thickness: linear, power-law, or exponential decay corresponds to regular diffusion, quasilocalization, or Anderson localization, respectively.^{3,9} Localization of classical waves in systems consisting of a collection of randomly oriented scattering objects has been observed using light,¹⁰ microwaves,¹¹ ultrasound,¹² and even water waves.¹³ Similarly, localization in quasicrystalline systems has been reported for light passing through Fibonacci dielectric multilayers.⁹ Recent experimental systems that have enabled observations of localization effects include light inside randomly modulated periodic¹⁴ and quasiperiodic¹⁵ photonic bandgap materials, as well as matter waves inside random optical potentials.^{16,17} Notably, using an ultracold atomic gas expanding into a disordered potential, it has been possible to observe three-dimensional Anderson localization.¹⁸

Here, we present a systematic study of wave propagation in three types of one-dimensional finite structures: periodic, quasiperiodic, and random. For each type of lattice, we compute the quantum mechanical transmission probability using a simple, yet accurate, numerical method. Finite or “local” systems are relevant in many practical situations, when only a small number of lattice elements are present, and their analysis has been shown useful in introducing the physics of wave propagation in finite media to the student classroom.^{19,20} We continue to use this pedagogical approach to show how the impressive effects of wave localization naturally emerge in non-periodic structures as the number of lattice sites considered is systematically increased. We begin by introducing the method used to compute the transmission coefficient, and consider first the periodic potential case, where we discuss the appearance of allowed and forbidden bands as the system size becomes infinite. Transport in the quasiperiodic and random lattices is then analyzed, providing insight into effects of disorder in the transmission vs. energy diagrams, from which wave localization results immediately follow.

II. STATEMENT OF THE PROBLEM

We consider the quantum mechanical problem of a particle of mass m and energy E incident from the left on a one-dimensional region where the potential $V(x)$ is nonzero only

within the finite interval $[a, b]$. The general solution to the time-independent Schrödinger equation,

$$-\frac{\hbar^2}{2m} \frac{d^2}{dx^2} \Psi(x) + V(x)\Psi(x) = E\Psi(x), \quad (1)$$

in this case is

$$\Psi(x) = \begin{cases} Ae^{ik_0x} + Be^{-ik_0x} & x < a \\ \Psi_{ab}(x) & a < x < b \\ Ce^{ik_0x} & x > b, \end{cases} \quad (2)$$

where $k_0 = \sqrt{2mE}/\hbar$. The terms Ae^{ik_0x} and Be^{-ik_0x} correspond to incident and reflected waves, respectively, and Ce^{ik_0x} corresponds to the transmitted wave.¹ The transmission coefficient is $T = |C/A|^2$.

Using a matrix approach, Griffiths and Steinke thoroughly analyzed the propagation of waves in locally periodic media and derived closed-form results for an arbitrary number of identical lattice sites.²⁰ Here, to find T for arbitrary potentials, we use the alternative and simple method introduced by Khondker and colleagues, which is based on the concept of generalized impedances.²¹ In this method, an analogy is drawn between quantum transport and wave propagation inside electrical transmission lines. Briefly, consider the potential step consisting of two regions with constant potential values V_1 ($x < 0$) and V_2 ($x > 0$). The quantum reflection coefficient is given by

$$R = \left| \frac{k_2 - k_1}{k_2 + k_1} \right|^2, \quad (3)$$

where $k_i = \sqrt{2m(E - V_i)}/\hbar$, $i = 1, 2$. In the case of voltage and current waves propagating through transmission lines [see Fig. 1(a)], the reflection coefficient due to an impedance mismatch is given by

$$R_L = \left| \frac{Z_{\text{LOAD}} - Z_{0,\text{LINE}}}{Z_{\text{LOAD}} + Z_{0,\text{LINE}}} \right|^2, \quad (4)$$

where Z_{LOAD} and $Z_{0,\text{LINE}}$ are the load and characteristic impedances of the transmission line, respectively.²² By comparing these two systems, Khondker and colleagues show that the quantum wavefunction, the derivative of the wavefunction, and the quantum current density correspond to the electrical current, the voltage, and the average power in a transmission line, respectively. Therefore, it is possible to associate a logarithmic derivative of the wavefunction with the ratio of voltage and current, thus defining the quantum mechanical impedance,

$$Z(x) = -\frac{i\hbar}{m} \frac{1}{\Psi(x)} \frac{d}{dx} \Psi(x). \quad (5)$$

To make operational use of this analogy, any arbitrary potential is first approximated by N segments, each with a potential value V_i ($i = 1, \dots, N$) that is regarded as constant. For a given E , each segment has a characteristic impedance,

$$Z_{0,i} = -\frac{i\hbar k_i}{m}, \quad (6)$$

which will contribute to the overall impedance of the whole transmission line. The input impedance at the beginning of the i th segment is calculated using²¹

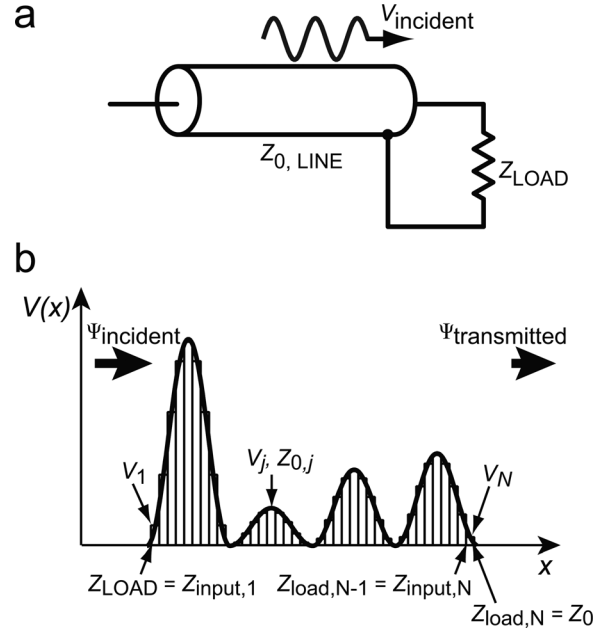


Fig. 1. Schematic of the generalized impedance method used to compute quantum transmission over a finite potential barrier. (a) An electrical transmission line of characteristic impedance $Z_{0,\text{LINE}}$ is terminated with a load impedance Z_{LOAD} . A wave of amplitude V_{incident} travelling to the right will undergo reflection at the connection point. The amplitude of the reflected wave is given by Eq. (4). (b) In the quantum mechanical problem of transmission across a potential barrier, the generalized impedance method regards the potential (thick solid line) as the load impedance Z_{LOAD} . To compute transmission, the potential barrier is approximated by N segments of equal width (thin bars, $V_1 \dots V_N$). Each segment (V_j) has a characteristic impedance ($Z_{0,j}$). Starting with the load impedance corresponding to the N th segment ($Z_{\text{load},N}$), the input impedance of the N th segment ($Z_{\text{input},N}$) is computed using Eq. (7), which in turn is taken as the load impedance of segment $N - 1$ ($Z_{\text{load},N-1}$). Then, an iterative procedure is followed until the load impedance of the whole potential barrier (Z_{LOAD}) is found. Finally, the quantum reflection coefficient can be found by substituting Z_{LOAD} and the characteristic impedance $Z_{0,\text{LINE}} = Z_0$ into Eq. (4). See text for details.

$$Z_{\text{input},i} = Z_{0,i} \frac{Z_{\text{load},i} \cosh(k_i l_i) - Z_{0,i} \sinh(k_i l_i)}{Z_{0,i} \cosh(k_i l_i) - Z_{\text{load},i} \sinh(k_i l_i)}, \quad (7)$$

where $Z_{\text{load},i}$ is the load impedance at the end of the i th segment and l_i is the length corresponding to the i th segment, as shown in Fig. 1(b). To determine the overall load and characteristic impedances of the complete potential, the following iterative procedure is followed. Starting with the characteristic impedance of the rightmost section ($Z_0 = -i\hbar k_0/m$) as the initial load ($Z_{\text{load},N}$), the input impedance at the beginning of segment N is calculated using Eq. (7), yielding $Z_{\text{input},N}$. Next, the N th input impedance is set as the $(N - 1)$ th load impedance ($Z_{\text{load},N-1} = Z_{\text{input},N}$) and the input impedance at the beginning of segment $N - 1$ is calculated using Eq. (7) again. This process is repeated until the input impedance of the first segment ($Z_{\text{input},1}$) is obtained. Finally, the reflection coefficient for the complete transmission line is found by equating $Z_{\text{LOAD}} = Z_{\text{input},1}$ and $Z_{0,\text{LINE}} = Z_0$, and substituting into Eq. (4). The quantum mechanical transmission coefficient is $T = 1 - R_L$.

III. TRANSMISSION IN A PERIODIC LATTICE

We begin by considering a periodic potential on a finite interval consisting of M identical lattice sites (a locally periodic potential),

$$V(x) = \begin{cases} (V_0/2)(\cos[(2\pi/\lambda)(x - \lambda/2)] + 1) & 0 \leq x \leq M\lambda \\ 0 & x < 0 \text{ or } x > M\lambda, \end{cases} \quad (8)$$

where λ is the period length and V_0 is the peak-to-peak amplitude (see Fig. 2). It is convenient to introduce the dimensionless variable $q = E/U$ for the energy, where $U = \hbar^2/(2m\lambda^2)$ is the “natural” unit of energy. In this paper, the parameter V_0 is taken as equal to U , as we found this is a good magnitude to illustrate the emergence of allowed and forbidden bands in the periodic case and the appearance of localization effects from the introduction of disorder.

Figure 2 presents the results for the transmission coefficient as a function of q when the number of lattice sites is varied. As M increases, three main features are to be noticed from these graphs. First, a sharp resonance peak appears at $q \sim 0.5$ when $M=2$. This is expected, as two lattice barriers in our potential define a single well, and the peak at $q \sim 0.5$ is due to resonant tunneling to the lowest, localized quasi-bound state of the well. Indeed, expansion of the potential well in a Taylor series around $x_0 = \lambda$ results in $V(x) \simeq (V_0/4)(2\pi/\lambda)^2(x - \lambda)^2$. The correspond-

ing energy levels are $\epsilon_n/U = \sqrt{V_0/U}(n + 1/2)$, from where $\epsilon_0/U = 1/2$, when $V_0/U = 1$. Second, there is an emergence of allowed energy bands where the transmission coefficient oscillates rapidly between 1 and lower but finite values, separated by forbidden bands where the transmission coefficient tends toward zero for large M . These features, as has already been pointed out,¹⁹ are precursors of the familiar band structure of infinitely periodic lattices, evident even for small numbers of lattice sites ($M \simeq 20$). Third, the number of transmission peaks or states in each band, as energy bands develop, is equal to $M - 1$. This is consistent with the expected result for large crystals ($M \gg 1$), where the number of states per band is M .²³ The expected gap between the first allowed energy band and the second one is $E_g = V_0/2$, also consistent with our numerical example ($E_g/V_0 \simeq 0.5$).

The locally periodic result can be directly compared with the result from the actual band structure that is easily obtained for an infinitely periodic lattice. To do this, we consider the Schrödinger equation with the potential of Eq. (8), now valid for all x

$$-\frac{\hbar^2}{2m} \frac{d^2}{dx^2} \Psi(x) + ((V_0/2) \times (\cos[(2\pi/\lambda)(x - \lambda/2)] + 1) - E) \Psi(x) = 0. \quad (9)$$

Using U and q , defined before, together with the change of variables

$$z = (\pi/\lambda)(x - \lambda/2), \quad (10)$$

$$a = 4(E/U - q/2), \quad (11)$$

reduces Eq. (9) to the canonical form of the Mathieu equation,²⁴

$$\frac{d^2}{dz^2} \Psi(z) + (a - 2q \cos(2z)) \Psi(z) = 0. \quad (12)$$

The solutions $\Psi(z)$ are of the Bloch form: $\Psi(z) = e^{ikz} w(z)$, where k is the normalized crystal momentum and $w(z)$ is periodic with period π . The characteristic values of a (corresponding to the energies, for a given value of q) can be found using standard, built-in routines of computational software programs (such as Mathematica’s `MathieuCharacteristicA`, which is the one used here). Figure 3 shows the resulting dispersion (energy versus normalized crystal momentum) graph (taking $V_0/U = 1$) in the reduced-zone scheme. The energy dispersion curves correspond to allowed energies, and therefore define energy bands where the transmission coefficient T is nonzero. Likewise, as the energy dispersion curves approach the edges of the Brillouin zone ($k = \pm 1$) there are band gaps, regions where $T = 0$. Figure 4 compares the results from the numerical computation corresponding to the finite lattice and the T vs. E diagram derived from the Mathieu equation. The energy band structure for the locally periodic potential is a

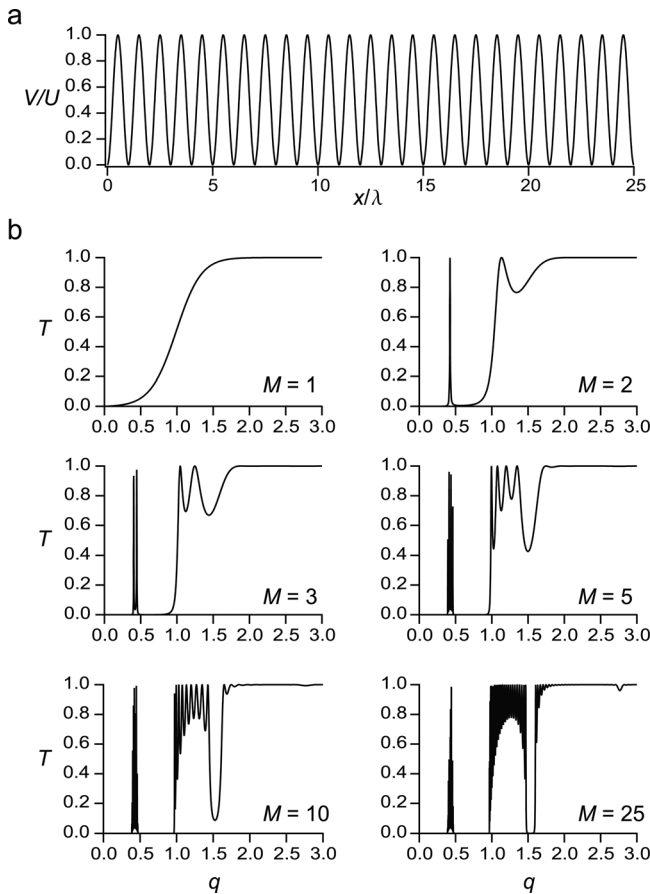


Fig. 2. Quantum transmission in a finite, periodic lattice. (a) The finite, periodic lattice considered, consisting of $M=25$ lattice sites in this case. (b) The transmission coefficient T as a function of the dimensionless parameter q , for an increasing number of lattice sites. See text for discussion of results. To compute quantum transmission, each lattice site was divided into $N = 100$ segments, and 3000 energy points were computed for each graph.

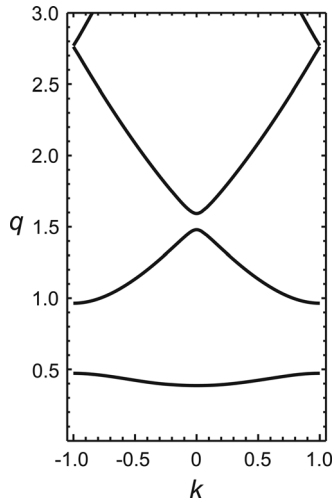


Fig. 3. Energy band diagram corresponding to an infinite, periodic potential. The characteristic values of the Mathieu equation (q , thick solid lines) are displayed as a function of the quasimomentum (k) in the reduced-zone scheme. The resulting energy levels define the familiar band structure. See text for details.

precursor of the resulting band structure for the infinitely periodic lattice.

IV. TRANSMISSION IN A QUASIPERIODIC LATTICE

We construct a locally quasiperiodic potential by taking the locally periodic potential of Eq. (8) and modulating the amplitudes of the lattice sites in a quasiperiodic fashion. To do this, we multiply the peak-to-peak amplitude V_0 of each lattice site by either 0 or 1, such that these multiplicative factors form a quasiperiodic, Fibonacci sequence X_n (see Fig. 5). The sequence X_n is thus composed of a succession of 0's and 1's that can be found using the following rule:²⁵

$$X_{n+1} = X_n X_{n-1}, \quad (13)$$

where the X 's are sequences of numbers and the operation of the right-hand side of the equation is concatenation, as in the following examples:

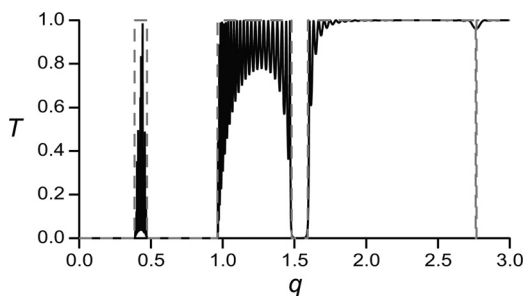


Fig. 4. Comparison of quantum transmission for finite and infinite periodic lattices. The quantum transmission coefficient T is displayed as a function of the normalized energy q for finite (black, solid line) and infinite (gray, dashed line) periodic potentials. The finite potential consisted of $M=30$ lattice sites, with each lattice site divided into 100 segments, and 3000 energy points were computed within the interval shown; the infinite potential result was derived from the energy band diagram of Fig. 3.

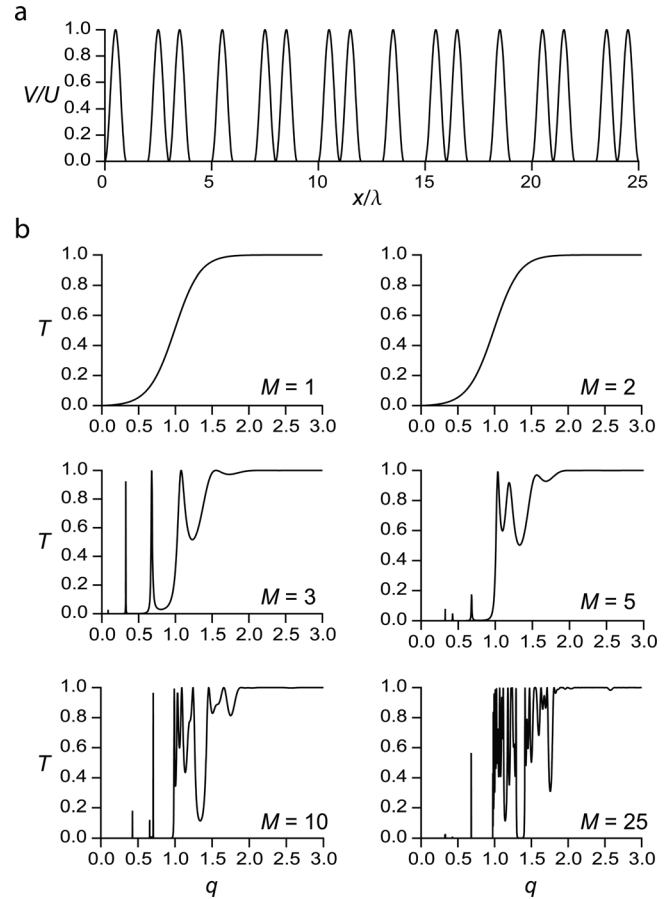


Fig. 5. Quantum transmission in a finite, quasiperiodic lattice. (a) The finite, quasiperiodic lattice considered, consisting of the first $M=25$ lattice sites. (b) The transmission coefficient T as a function of the dimensionless parameter q , for an increasing number of lattice sites. See text for discussion of results. To compute quantum transmission, each lattice site was divided into 100 segments, and 3000 energy points were computed for each graph.

$$\begin{aligned} X_0 &= \{1\}; \\ X_1 &= \{1, 0\}; \\ X_2 &= X_1 X_0 = \{1, 0, 1\}; \\ X_3 &= X_2 X_1 = \{1, 0, 1, 1, 0\}; \\ X_4 &= X_3 X_2 = \{1, 0, 1, 1, 0, 1, 0, 1\}; \\ X_5 &= X_4 X_3 = \{1, 0, 1, 1, 0, 1, 0, 1, 1, 0, 1, 1, 0\}. \end{aligned} \quad (14)$$

The length of each sequence X_n is given by the Fibonacci numbers, 1, 2, 3, 5, 8, 13, ... The sequences X_n present many regularities: they are self-similar (redefining $\{1, 0\} \rightarrow \{1\}$ and $\{1\} \rightarrow \{0\}$ in a given X_n produces X_{n-1}); the ratio of the total number of 1's to the number of 0's in a given X_n approaches the golden mean $\tau = 1 + 1/\tau = (\sqrt{5} + 1)/2 \approx 1.618$ as n increases; and wave scattering from structures based on Fibonacci sequences produces a spectrum filled in a dense fashion, with sharp peaks whose spacing is related to the golden mean (see Fig. 8).^{5,6,25} The sequence X_n is quasiperiodic, meaning that it is periodic in a higher-dimensional space (the sequence arises from the projection of a two-dimensional periodic structure into one dimension).^{5,25}

We computed the transmission versus energy curves for increasing numbers of lattice sites (see Fig. 5). As in the periodic case, it is possible to identify initial resonances with the known energy levels of approximated potentials. The

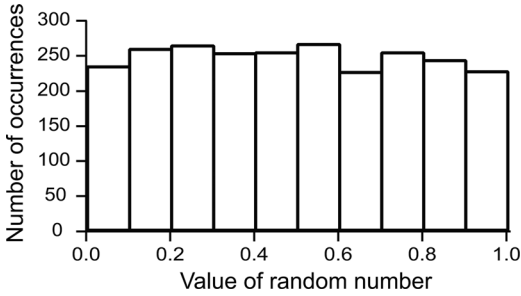


Fig. 6. Distribution of random numbers used to generate the random potential. To generate the set of pseudo-random numbers that are used to define the amplitudes of the lattice sites in the random potential, the IgorPro command `SetRandomSeed` was set to 0.038 and the built-in routine `noise()` was used. A histogram corresponding to the first 2500 numbers generated shows a uniform distribution.

case $M = 3$ can be approximated as the infinite potential box of width 2λ , whose associated energy levels are $\epsilon_n = h^2 n^2 / (32m\lambda^2) = Un^2/16$. The first four levels (at normalized energy values near 0.0625, 0.25, 0.56, and 1.0) can be identified in the transmission curve.

As the number of lattice sites increases, the resulting transmission curves develop a structure that seems to have

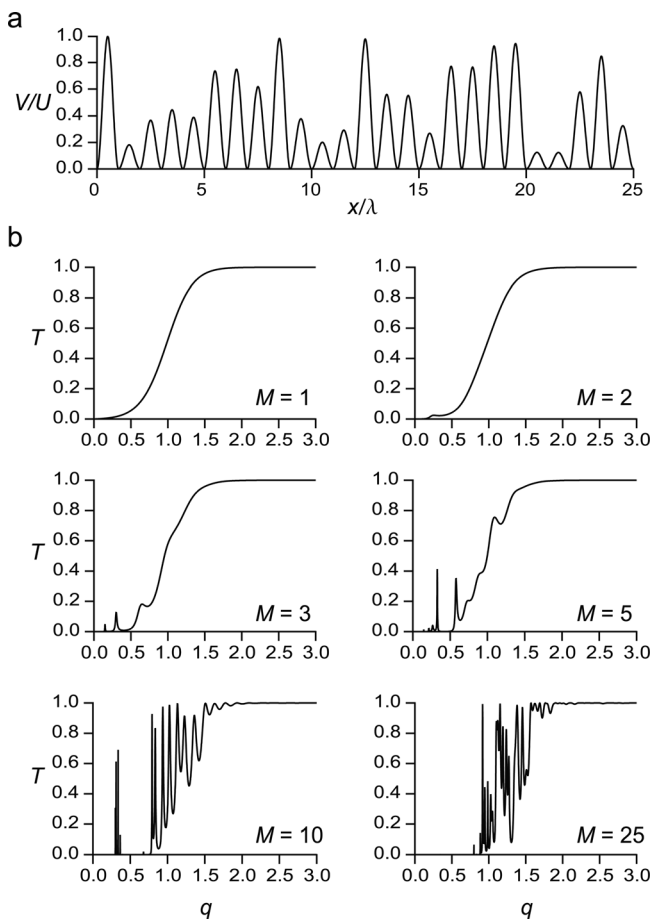


Fig. 7. Quantum transmission in a finite, random lattice. (a) The finite, random lattice considered, consisting of the first $M = 25$ lattice sites. (b) The transmission coefficient T as a function of the dimensionless parameter q , for an increasing number of lattice sites. See text for discussion of results. To compute quantum transmission, each lattice site was divided into 100 segments, and 3000 energy points were computed for each graph.

energy bands and bandgaps. Indeed, theory and experiments on light propagation through Fibonacci dielectric multilayers have found that increasing the number of layers has the effect of suppressing transmission in certain wavelength regions, which have been called “pseudo band gaps” (to distinguish from true band gaps of periodic media).^{9,26,27} However, the transmission regions corresponding to energy “bands” are not uniform. In fact, they consist of a rich structure that is expected to be fractal or self-similar. This last property has been experimentally demonstrated (when a condition to maximize the quasiperiodicity of the system is satisfied).⁹

V. TRANSMISSION IN A RANDOM LATTICE

We generate the locally random potential by again taking the locally periodic lattice, Eq. (8), and multiplying the peak-to-peak amplitude of the i th lattice site now by a random number that is between 0 and 1. The built-in routine `noise()` of the statistics software IGORPRO was used to generate a set of evenly distributed, pseudo-random numbers (distribution shown in Fig. 6), while the routine `SetRandomSeed` was used to obtain repeatable pseudo-random numbers.

Figure 7 shows the resulting lattice, together with the corresponding transmission vs. energy diagrams for a varied number of lattice sites ($M \leq 25$). Contrary to the periodic and quasiperiodic cases, there is no obvious emergence of energy “gaps” or “pseudo-gaps.” Instead, initial resonance peaks at small energies in the transmission probability progressively disappear when the number of lattice sites considered is increased. This trend is confirmed by computing

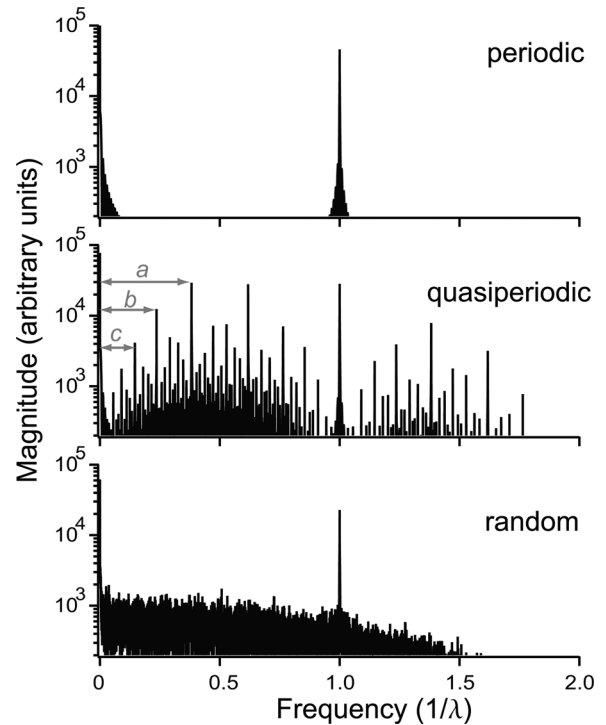


Fig. 8. Fourier transform of the periodic, quasiperiodic, and random potentials. A clear transition from a single frequency peak to a floor of noise is observed as the degree of disorder is increased. For the quasiperiodic lattice, the ratio $a/b = b/c = \dots$ is equal to the golden mean, reflecting the fractal nature of this structure. To compute the corresponding Fourier transforms, a total of $M = 2500$ lattice sites were considered in each case.

transmission coefficients for $M > 25$ (see Fig. 9). We come back to this point in the next section, when discussing localization effects.

It is instructive to contrast the Fourier transform of the random potential with the periodic and quasiperiodic cases (see Fig. 8). As expected, the periodic case produces a single peak centered at the reciprocal of the lattice constant ($1/\lambda$). This single peak establishes a well-defined condition for Bragg diffraction during wave propagation. Although this peak is also present in some degree for the other potentials (reflecting the fact that we chose to have the same lattice site length, λ , for all types of structures), there are dominant features that are lattice-specific. For a quasiperiodic lattice, a multitude of well-defined, closely spaced peaks appear, with positions that are related through the golden mean ratio.⁶ The presence of resonances indicates that, during wave propagation, a process similar to Bragg diffraction is also expected to occur here, although the resulting diffracted spots are weaker and more densely spaced compared to the periodic case. Finally, the random lattice has a Fourier transform that, apart from the aforementioned peak corresponding to the lattice site spacing, is characterized by a continuum of “noise.” Nothing similar to Bragg diffraction is expected to occur here, because resonances (a mechanism that can enhance wave transmission) are suppressed. These features

directly lead to the emergence of wave localization effects as the lattice changes from periodic to non-periodic.

VI. WAVE LOCALIZATION

The behavior of the transmission coefficient as a function of incident energy is clearly distinct for the three types of finite lattices presented here: periodic, quasiperiodic, and random, when the number of lattice sites is small ($M < 30$). When M is further increased in the computation of quantum transmission ($M = 50 \dots 500$, see Fig. 9), we confirm that significant differences remain, offering a perspective to appreciate effects of the transition from order to disorder. In the periodic potential case, the resulting energy band structure is evident, becoming better defined as M increases. In contrast, the transmission coefficient for the random lattice does not show any allowed energy bands separated by forbidden bands, irrespective of the value of M . An intermediate behavior corresponds to the quasiperiodic lattice, where a band structure (or the precursor thereof) is observed for small energies and low M , but gradually disappears as M increases. This latter behavior helps to illuminate one aspect of why the term “pseudo band gap” is used for quasiperiodic lattices: within the context of finite lattices, the band gaps do exist

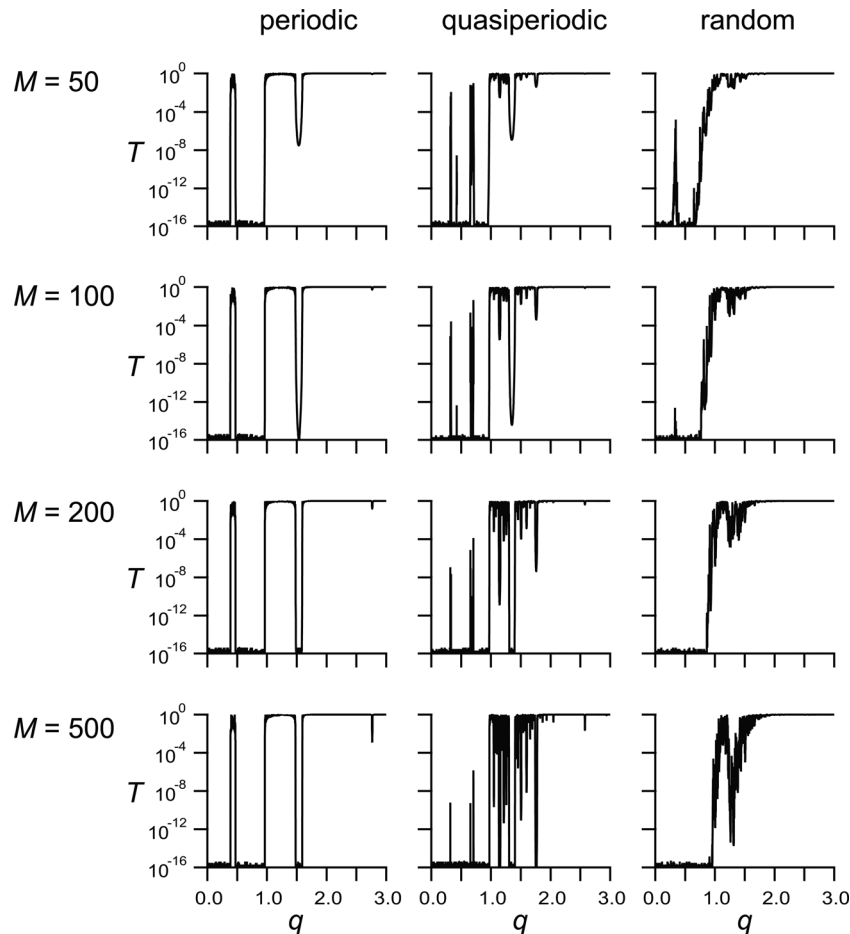


Fig. 9. Quantum transmission coefficient behavior for the periodic, quasiperiodic, and random finite lattices in the case of large numbers of lattice sites. The periodic potential case shows a clear energy band structure that is well-defined in all cases. In contrast, the quasiperiodic case does display energy band gaps, but they tend to disappear when M is increased. Although weak resonances can be appreciated for the random case, there is no evidence of an energy band structure. These characteristics help understand localization effects (see text). To compute quantum transmission, each lattice site was divided into 100 segments, and 3000 energy points were computed for each graph.

but become less defined as more lattice sites are involved in transmission.

The qualitative characteristics of transmission discussed above provide us with the starting point to present quantitative results on localization effects in non-periodic potentials. From the discussion presented in the Introduction, increasing the number of lattice sites of a random, one-dimensional potential should lead to exponential decay of the transmission coefficient. To demonstrate this behavior, we compute the average of the transmission coefficient within a given interval of energies and display it as a function of the number of lattice sites M (the “average transmissivity” concept discussed in Ref. 28). These conditions correspond to calculating the total transmission coefficient of a wavepacket, square-shaped in energy space, incident on a 1D potential (such a wavepacket could be prepared, for example, with light passing through a band-pass filter). We also assume that each spectral component of the wavepacket travels independently of any other component. To avoid effects of trivial, classical “localization,” we consider exclusively energies above the maximum potential barrier height contained within the overall potential.

Transmission coefficients averaged over the energy interval $q = [1, 2]$ are shown in Fig. 10, with M varied between 1 and 5000, demonstrating the appearance of wave localization

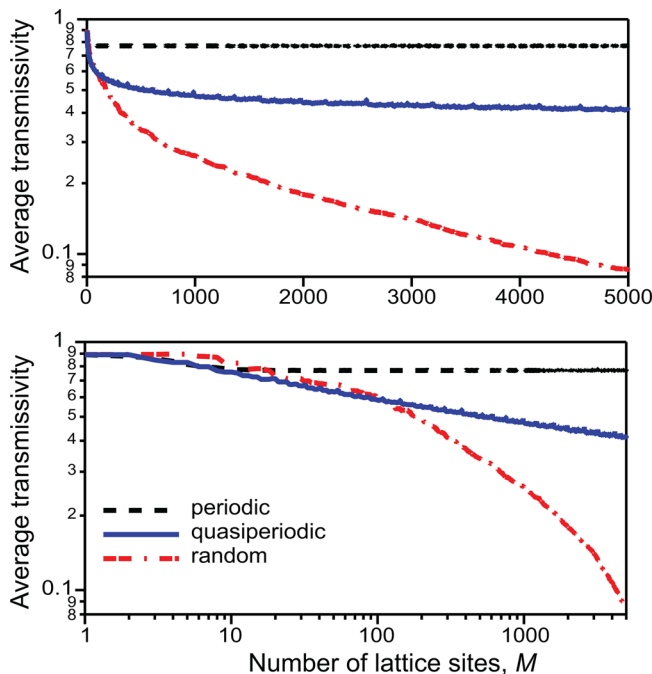


Fig. 10. (Color online) Emergence of localization effects for the quasiperiodic and random lattices. Transmission coefficients averaged over the energy interval $q = [1, 2]$ are shown with M varied between 1 and 5000, for the periodic (black, dashed line), quasiperiodic (blue, solid line), and random (red, dashed-point line) finite lattices. In the cases of the quasiperiodic and random potentials the transmissivity decreases monotonically as the number of lattice sites is increased. Decay is consistent with power-law (quasiperiodic potential) and exponential (random potential) dependence, as evidenced by the same results displayed in log-linear (top graph) and log-log (bottom graph) scales. The average transmissivity for the periodic lattice remains constant beyond $M \approx 10$ —identifying a point at which the finite periodic lattice can be regarded as a sufficient approximation to its infinite counterpart. In all cases $V_0/U = 1$ was used. To compute quantum transmission in all cases, each lattice site was divided into 100 segments, and 4000 equally spaced energy points within the interval $E/U = [1, 2]$ were used to determine the average transmissivity.

for both quasiperiodic and random potentials. The energy interval considered covers parts of the second and third energy bands for the periodic potential case (see Fig. 4). This choice avoids trivial localization (by using $q \geq 1$), captures significant variations in the transmissivity curves for the number of lattice sites considered (see Fig. 9), and optimizes signal to noise of the average transmissivity. Averaging for energies significantly greater than the heights of the potentials increases the localization size, such that it becomes impractical to observe in these finite models.

The transmission curve for the random potential decreases exponentially as M is increased, and data are well fit using two decay length constants: $M_1 = 170$ and $M_2 = 2060$ (fitting not shown). More than one decay constant is involved because of the averaging of the transmission coefficients over a relatively broad energy interval ($q = [1, 2]$). In the quasiperiodic potential case, data within the range $M = [2, 5000]$ are well fit by a simple power-law function, with exponent $b = -0.15$ (fitting not shown). The specific values of M_1 , M_2 , and b are dictated by how the transmission curves are affected within the averaged region as M increases. For example, the transmission curve for the random lattice (see Fig. 9) shows the onset of a marked decrease around $q = 1$ that starts when $M \approx 200$, thus explaining the value of M_1 found in our case.

The transmission for the periodic case in Fig. 10 is independent of the number of lattice sites. This implies unimpeded transmission, which is consistent with electronic wave functions propagating in a perfect periodic lattice. By contrast, for the random potential, Anderson localization is observed. Localization is caused by above-the-barrier reflection and wave interference in the non-periodic structures. Finally, it is striking to observe that the quasiperiodic lattice also leads to localization—in this case “slower” than exponential. Therefore, our computation helps identify the difference between power-law localization (corresponding to the quasiperiodic potential) and exponential or “true” Anderson localization. The term “weak localization” is also used in the literature, simply meaning that the localization length exceeds all other characteristic lengths of the system.²⁹

The average transmission computed for the quasiperiodic potential displays an additional, remarkable effect: the appearance of a series of resonance peaks, occurring at the Fibonacci values $M = 1, 2, 3, 5, 8, 13, \dots$ (see Fig. 11). Furthermore,

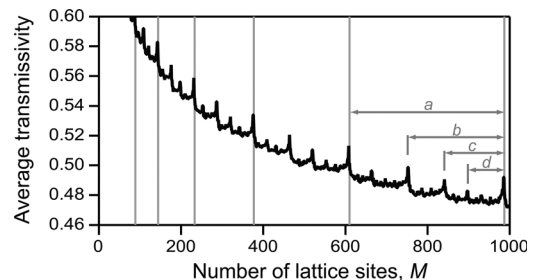


Fig. 11. Self-similar resonances in the average transmissivity for the quasiperiodic potential. The average transmissivity (black line) shows a number of resonance peaks located wherever the number of lattice sites is equal to a Fibonacci number (gray vertical lines, only lines corresponding to $M = 89, 144, 233, 377, 610, 987$ are shown). Additionally, smaller peaks can be distinguished between Fibonacci lines. All of the resonances locate at positions that define distances (arrowed, horizontal gray lines) that are related through the self-similarity property $a/b \approx b/c \approx c/d \approx (\sqrt{5} + 1)/2 \approx 1.618$ characteristic of the Fibonacci sequence.

smaller, additional resonances can be discerned between the main ones. All of the resonances distinguished are located at positions that satisfy the Fibonacci condition: the ratio of one Fibonacci value divided by its predecessor approximates the golden mean. These resonances, which arise due to wave interference, highlight the existence of long-range order in quasiperiodic structures, and reflect the self-similarity properties of the underlying Fibonacci series. It can be inferred from these observations that a quasiperiodic lattice is a true intermediate between order and disorder, presenting wave localization effects as well as the emergence of well-defined resonances in a transmission spectrum.

VII. CONCLUSIONS AND FINAL REMARKS

We have presented a systematic approach to wave propagation in periodic and non-periodic lattices. Using a simple numerical method based on the analogy with electrical signals propagating in transmission lines, the quantum mechanical transmission probability was computed for finite lattices. The band structure characteristic of crystals was recovered for a periodic potential, and the corresponding average transmission was shown to be independent of the number of lattice sites considered. These results provide a reference for comparison with subsequent analysis of non-periodic lattices. When wave transmission in a quasiperiodic, Fibonacci lattice was considered, the concepts of “quasi band gap,” self-similarity, and quasi-localization naturally emerged. Finally, the random potential case allowed for a simple, numerical observation of Anderson localization. This approach should provide students insight into how transport properties in finite media behave as non-periodicity or randomness is introduced. As has been emphasized,³ the extraordinary phenomenon of localization is a general property of wave propagation that results from interference effects during transmission— aspects whose consequences can be followed in the computation of transmission coefficients. A possible extension to this study includes considering potentials with various degrees of randomness or quasiperiodicity. Classroom experiments using transmission of electronic signals across cable lines³⁰ could provide a framework to observe localization effects and to compare with numerical computation results. The numerical method used here to calculate quantum transmission probabilities is general enough to be applied by students to a wide variety of physical situations involving wave propagation through arbitrary one-dimensional structures.

ACKNOWLEDGMENTS

This work was supported by CONACYT through grants Repatriados-2009 (S-4130) and Fondos Sectoriales-SEP-2009 (S-3158). The author thanks Dr. Paul Riley, Dr. Kirk Madison, and anonymous reviewers for a careful reading of the manuscript.

^{a)}Electronic mail: bgutierrez@ipicyt.edu.mx

¹Eugen Merzbacher, *Quantum Mechanics*, 2nd ed. (Wiley, New York, 1970).

²P. W. Anderson, “Absence of diffusion in certain random lattices,” *Phys. Rev.* **109**(5), 1492–1505 (1958).

³A. Lagendijk, B. van Tiggelen, and D. S. Wiersma, “Fifty years of Anderson localization,” *Phys. Today* **62**(8), 24–29 (2009).

- ⁴D. Shechtman, I. Blech, D. Gratias, and J. W. Cahn, “Metallic phase with long-range orientational order and no translational symmetry,” *Phys. Rev. Lett.* **53**(20), 1951–1953 (1984).
- ⁵C. Janot, J.-M. Dubois, and M. de Boissieu, “Quasiperiodic structures: Another type of long-range order for condensed matter,” *Am. J. Phys.* **57**(11), 972–987 (1989).
- ⁶N. Ferralis, A. W. Szmodis, and R. D. Diehl, “Diffraction from one- and two-dimensional quasicrystalline gratings,” *Am. J. Phys.* **72**(9), 1241–1246 (2004).
- ⁷J. B. Sokoloff, “Unusual band structure, wave functions and electrical conductance in crystals with incommensurate periodic potentials,” *Phys. Rep.* **126**(4), 189–244 (1985).
- ⁸B. Sutherland and M. Kohmoto, “Resistance of a one-dimensional quasicrystal: Power-law growth,” *Phys. Rev. B* **36**(11), 5877–5886 (1987).
- ⁹W. Gellermann, M. Kohmoto, B. Sutherland, and P. C. Taylor, “Localization of light waves in Fibonacci dielectric multilayers,” *Phys. Rev. Lett.* **72**(5), 633–636 (1994).
- ¹⁰D. S. Wiersma, P. Bartolini, A. Lagendijk, and R. Righini, “Localization of light in a disordered medium,” *Nature* **390**(6661), 671–673 (1997).
- ¹¹A. A. Chabanov, M. Stoytchev, and A. Z. Genack, “Statistical signatures of photon localization,” *Nature* **404**(6780), 850–853 (2000).
- ¹²H. Hu, A. Strybulevych, J. H. Page, S. E. Skipetrov, and B. A. van Tiggelen, “Localization of ultrasound in a three-dimensional elastic network,” *Nat. Phys.* **4**(12), 945–948 (2008).
- ¹³P. E. Lindelof, J. Nørregaard, and J. Hanberg, “New light on the scattering mechanisms in Si inversion layers by weak localization experiments,” *Phys. Scr. T* **1986**, 17–26 (1986).
- ¹⁴T. Schwartz, G. Bartal, S. Fishman, and M. Segev, “Transport and Anderson localization in disordered two-dimensional photonic lattices,” *Nature* **446**(7131), 52–55 (2007).
- ¹⁵L. Levi, M. Rechtsman, B. Freedman, T. Schwartz, O. Manela, and M. Segev, “Disorder-enhanced transport in photonic quasicrystals,” *Science* **332**(6037), 1541–1544 (2011).
- ¹⁶G. Roati, C. D’Errico, L. Fallani, M. Fattori, C. Fort, M. Zaccanti, G. Modugno, M. Modugno, and M. Inguscio, “Anderson localization of a non-interacting Bose-Einstein condensate,” *Nature* **453**(7197), 895–898 (2008).
- ¹⁷J. Billy, V. Josse, Z. Zuo, A. Bernard, B. Hambrecht, P. Lugan, D. Clement, L. Sanchez-Palencia, P. Bouyer, and A. Aspect, “Direct observation of Anderson localization of matter waves in a controlled disorder,” *Nature* **453**(7197), 891–894 (2008).
- ¹⁸S. S. Kondov, W. R. McGehee, J. J. Zirbel, and B. DeMarco, “Three-dimensional Anderson localization of ultracold matter,” *Science* **334**(6052), 66–68 (2011).
- ¹⁹D. J. Griffiths and N. F. Taussig, “Scattering from a locally periodic potential,” *Am. J. Phys.* **60**(10), 883–888 (1992).
- ²⁰D. J. Griffiths and C. A. Steinke, “Waves in locally periodic media,” *Am. J. Phys.* **69**(2), 137–154 (2001).
- ²¹A. N. Khondker, M. R. Khan, and A. F. M. Anwar, “Transmission line analogy of resonance tunneling phenomena: The generalized impedance concept,” *J. Appl. Phys.* **63**(10), 5191–5193 (1988).
- ²²Giovanni Miano and Antonio Maffucci, *Transmission Lines and Lumped Circuits* (Academic, San Diego, 2001).
- ²³Charles Kittel, *Introduction to Solid State Physics*, 7th ed. (Wiley, New York, 1996).
- ²⁴Milton Abramowitz and Irene I. Stegun, *Handbook of Mathematical Functions* (Dover, New York, 1965).
- ²⁵Michael P. Marder, *Condensed Matter Physics* (Wiley, New York, 2000).
- ²⁶M. Kohmoto, B. Sutherland, and K. Iguchi, “Localization of optics: Quasiperiodic media,” *Phys. Rev. Lett.* **58**(23), 2436–2438 (1987).
- ²⁷D. S. Wiersma, R. Sapienza, S. Mujumdar, M. Colocci, M. Ghulinyan, and L. Pavesi, “Optics of nanostructured dielectrics,” *J. Opt. A, Pure Appl. Opt.* **7**(2), S190–S197 (2005).
- ²⁸P. Erdős, E. Liviotti, and R. C. Herndon, “Wave transmission through lattices, superlattices and layered media,” *J. Phys. D: Appl. Phys.* **30**(3), 338–345 (1997).
- ²⁹B. Kramer and A. MacKinnon, “Localization: Theory and experiment,” *Rep. Prog. Phys.* **56**(12), 1469–1564 (1993).
- ³⁰A. Hache and A. Slimani, “A model coaxial photonic crystal for studying band structures, dispersion, field localization, and superluminal effects,” *Am. J. Phys.* **72**(7), 916–921 (2004).